Ultrahigh-vacuum quasiepitaxial growth of model van der Waals thin films. I. Theory

S. R. Forrest and Y. Zhang*
Advanced Technology Center for Photonics and Optoelectronic Materials (ATC/POEM), Department of Electrical Engineering, Princeton University, Princeton, New Jersey 08544
(Received 24 November 1993)

We introduce a model to calculate the equilibrium crystal configuration of a monolayer lattice of large, planar organic molecules bonded to a substrate by van der Waals (vdW) forces. The model significantly simplifies analysis by replacing the conventional atom-atom vdW potential summation with a single ellipsoidal potential centered in the molecular plane. Our results indicate that recent observations of crystalline quasiepitaxial vacuum growth of incommensurate lattices of these planar molecular films result from the relatively large intralayer stiffness as compared to the interlayer shear stress. Good agreement between calculated and observed structures is achieved using no adjustable parameters. The model is used to predict molecular structures which are likely to form quasiepitaxial layers. Comparison with previous models describing physisorption of incommensurate layers of atomic vdW systems on graphite substrates is also made. In the subsequent paper (paper II) we present experimental data comparing the grown structures of several model compounds with the theoretical predictions made here.

I. INTRODUCTION

During the past few years, numerous organic and inorganic compounds bonded by the van der Waals (vdW) force have been deposited on a variety of substrates in crystalline thin film form.[1–14] Many of these films have exhibited the remarkable property that they are crystalline with very large grains, even though the overlayer is incommensurate with the substrate. This ability to grow such thin films without the necessity for lattice matching has variously been termed "van der Waals epitaxy," "quasiepitaxy," or "layered growth." More recently, experience in our own laboratory suggests that crystalline quasiepitaxial (QE) growth may be a general property of materials which are bonded primarily by vdW forces.[1,3,5] Due to the flexible nature of the vdW bond, the compressibility between molecules within a particular material layer is often considerably smaller than the compressibility (or shear stress) between molecules in the layer and substrate. Thus a crystalline sheet of a thin molecular van der Waals film can sometimes be grown with insufficient strain energy at the interface to induce defects. Furthermore, should the substrate have the same order of symmetry as the film, extended crystalline sheets of the thin film can be grown approximately oriented to the substrate even though lattice matching is not achieved. Hence quasiepitaxy can be defined as the approximate ordering of a crystalline layer to a substrate which is a result of the flexible, vdW-like bonds which are responsible for the layer adhesion.

Interest in this growth mechanism arises from the possibility for engineering a class of "crystalline" materials consisting of ordered multilayer structures of two or more vdW solids. Such multilayers have already been grown in several laboratories using the ultrahigh-vacuum process of organic molecular-beam deposition (OMBD).[2–6] These structures exhibit QE ordering as well as exciton confinement within the layered structure.[2,3] Organic multiple-quantum-well (MQW) structures, where the individual layers are in the range of 10–50 Å (i.e., comparable to the exciton radius) have potential application to nonlinear optical devices such as optical modulators, high efficiency optical sources for use in the visible and infrared spectral regions, high efficiency photodetectors such as photovoltaic cells, waveguides, and a wide range of other optoelectronic devices, many of which have already been demonstrated.[15–18] Therefore, the ability to engineer these QE thin films offers an unprecedented flexibility for the materials scientist to manipulate materials properties while at the same time having considerable control over the structure of the films.

The systems considered here are considerably different from previously studied lattice-mismatched physisorbed atomic and molecular systems[19–21] in that the *interlayer* compressibility of molecular heterointerfaces is far greater than the *intralayer* compressibility due to the spatial extent of the molecules. This is in contrast to atomic vdW systems where these quantities are comparable.[21] As will be shown, it is this asymmetry in elasticity which leads to layer orientation in crystalline organic thin-film systems.

We also note that QE is different from true epitaxy of organic monolayers which has been investigated widely in previous work.[22–24] Since the compressibility within the thin-film layer is less than the shear stress between the layer and the substrate (i.e., interlayer compressibility) in QE systems, the binding to the substrate provides a preferred orientational alignment between the thin film and the substrate lattices, although there is insufficient shear stress at the interface with the substrate to induce a high density of defects in the lattice-mismatched deposited molecular layer. Hence subsequent layers are grown in their relaxed, bulk structural configuration. On the other hand, *epitaxial* growth of molecular films which are more tightly coupled to such substrates as the alkali

 ©1994 The American Physical Society

halides or the metal chalcogenides forces the first adlayer to conform to the molecular spacing of the substrate.[22–24] Since this usually does not conform to the relaxed, bulk molecular structure, such epitaxial growth induces substantial strain into the subsequently grown layers. Hence, epitaxial growth of severely mismatched molecular systems has only been observed for monolayer coverage of the substrate. Further growth results in significant disorder, as will be shown in paper II.

It is the objective of this paper and the subsequent paper (paper II) to present a detailed theoretical framework and experimental basis for QE growth of archetype vdW-bonded molecular thin films. The model, which has been briefly outlined in previous work,[25] is calculationally simple in that it replaces the large number of pairwise atom-atom potentials which must be summed between adjacent molecules by a single, ellipsoidally symmetric molecule-molecule potential. The model is further simplified since it has no adjustable parameters. Our analysis provides a clear, qualitative understanding of the factors which lead to QE ordering of molecular thin films, and the results are consistent with experiment. The model is applied to structures employing the archetype planar molecules; 3,4,9,10 perylenetetracarboxylic dianhydride (PTCDA, $C_{24}O_6H_8$) and 3,4,7,8 naphthalenetetracarboxylic dianhydride (NTCDA, $C_{14}O_6H_4$), with results in good agreement with observation.

While other models have also been previously developed to understand epitaxial growth using approximations similar to those employed here (e.g., using the rigid-lattice approximation[26,27]), epitaxial systems are *inherently* different from QE systems. The primary difference lies in the incommensurability of QE layers with the substrate. Whereas one can model epitaxial growth by a harmonic potential with a period equal to the atomic spacing of the substrate,[27] incommensurate lattices cannot be treated as such since the potential between overlayer and substrate is anharmonic. Hence the analytical solutions which are attained for epitaxial systems are replaced here by computationally intensive methods. As will be shown, however, our choice of an approximate, "ellipsoidal potential" greatly simplifies the problem of modeling QE, therefore allowing us to rapidly determine the layer structure which is achieved for even the most complex planar molecular structures.

Extending the model to other molecules where the long-range Coulomb potential plays a role, as is the case with the phthalocyanines, significantly complicates the problem, and hence will not be considered here. However, the methods employed, in principle, can be extended to include these and other bonding forces (e.g., hydrogen bonding, ionic and covalent bonds, etc.), although these extensions make the prediction of crystal structure extremely calculationally time consuming. We therefore consider purely vdW-bonded molecular layers as *model systems* whose study enables the development of a qualitative picture of the primary factors involved in determining how crystalline order in QE layers can be obtained.

In paper II we present data concerning the microstructure of monolayer and multilayer films of these same archetype compounds (i.e., PTCDA and NTCDA), as well as of copper phthalocyanine (CuPc).[28] By examining the growth in vacuum of both single and multilayered structures consisting of these materials using a wide range of analytical tools including x-ray diffraction, scanning tunneling and electron microscopy, *in situ* reflection high-energy electron diffraction (RHEED), and optical birefringence, we experimentally observe the principal factors governing the growth of ordered, QE thin films, and compare these with our theoretical predictions which are in reasonable agreement.

The paper is organized as follows: In Sec. II we provide detailed bulk structural information for the two molecules under investigation. These data are essential for considering the structure of the thin films. This is followed in Sec. III by a general discussion of the criteria for quasiepitaxy. In Sec. IV we present the results of calculations involving monolayer growth of organic films on different substrate structures. We also include a discussion of the general applicability of the theory to molecular organic thin-film systems. In Sec. V we compare our results to other, previous models of physisorption of vdW-bonded atoms on graphite substrates, and in Sec. VI we present conclusions.

II. CRYSTAL STRUCTURE

The compound PTCDA grows in a monoclinic lattice structure in the $P2_1/c(C_{2h}^5)$ space group. The molecular configuration, as well as two perspective views of the *bulk* structure of PTCDA as determined by x-ray diffraction, are shown in Fig. 1(a). The unit-cell lattice constants are $a=3.72$ Å, $b=11.96$ Å, and $c=17.34$ Å, and the lattice angle is $\beta=98.8°$. Molecules in a stack are offset in the stacking direction due to an 11° tilt with respect to the substrate plane.[1,29] The unit cell of NTCDA [see Fig. 1(b)] is in the same $P2_1/c(C_{2h}^5)$ space group as PTCDA. The cell parameters are measured by x-ray diffraction to be $a=7.89$ Å, $b=5.33$ Å, and $c=12.74$ Å with a lattice angle of $\beta=109.04°$.

III. CRITERIA FOR QUASIEPITAXY

The primary requirement for QE is that there exists a range over which a surface molecule can be translated relative to the substrate without significantly changing the system energy. If the potential between molecules within a layer is ϕ_{intra}, and between molecules in different layers is ϕ_{inter}, then this condition is related to the magnitudes of the interlayer and intralayer compressibilities (or elasticities) via $\phi_{\text{intra}}'' \gg \phi_{\text{inter}}''$, where ϕ'' is the second spatial derivative of ϕ along the various crystalline directions and angles. That is, ϕ'' is the elastic constant of the lattice along a particular direction. This condition for QE is independent of the relative magnitudes of the crystal binding energies, ϕ_{intra} or ϕ_{inter}. As in many cases involving large planar molecules, $\phi_{\text{inter}} > \phi_{\text{intra}}$, while $\phi_{\text{inter}}'' \ll \phi_{\text{intra}}''$. This differs from atomic vdW systems where there is no strict adherence to these conditions.[21]

The crystalline compressibility has been examined by

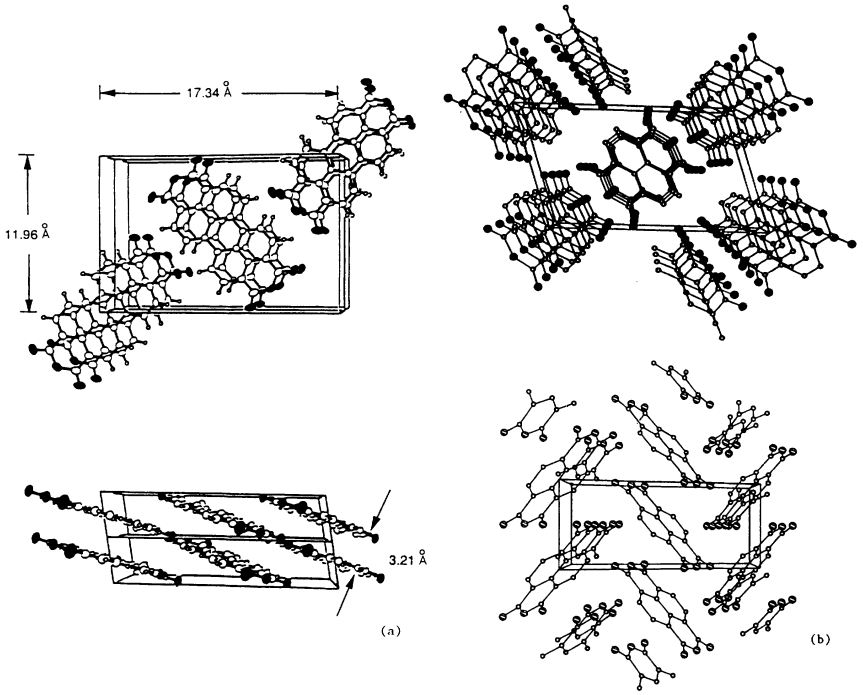

FIG. 1. Two perspective views of a molecule of (a) PTCDA and (b) NTCDA.

calculating the vdW bond energy between two-dimensional (2D) interfaces of PTCDA and NTCDA using the atom-atom potential method.[30] Here, the total bond potential is given by $\Phi=\Sigma\phi_{ij}$, where ϕ_{ij} is the potential between the ith and jth *atoms* in the two molecules which is found using

$$\phi_{ij}=-\alpha_{ij}/r_{ij}^6+\beta_{ij}\exp(-\gamma_{ij}r_{ij}) . \quad (1)$$

The radial distance between atoms i and j in different molecules is r_{ij}, and α, β, and γ are vdW constants[31,32] for each pair of constituent atoms in the two molecules. The minimum energy corresponding to the equilibrium crystal configuration is obtained when $\Phi'=0$ and $\Phi''>0$.

There are several assumptions made when applying the atom-atom potential procedure: (i) The model is static. That is, the calculation applies to equilibrium at $T=0$ K, and hence it cannot predict dynamic growth processes, nor does it consider vibrational contributions at $T>0$. Typically, these latter effects are small compared with Φ; (ii) the vdW forces are isotropic, and are not significantly perturbed by the molecular structure; (iii) the molecules are rigid; and, as noted above, (iv) there is no significant contribution to the intermolecular energy arising from Coulombic forces, higher-order multipoles, etc. Previous calculations for nonpolar molecules[30] such as those studied here have shown that these assumptions are generally valid.

As a test of the accuracy of the method, we have calculated several aspects of the bulk crystal structure of PTCDA, and compared these results with x-ray crystallographic data. We note that calculation of the full bulk structure is a complex 3D problem involving numerous degrees of freedom between the several molecules in the cells. Hence, in this part of the study, only limited aspects of the 3D structure are calculated to test the model accuracy. As will be shown below, calculating 2D structures is considerably simpler.

In Fig. 2 we show the energy of two organic molecules stacked one above the other, and translated in a plane normal to the stacking direction. Values for the vdW coefficients used are listed in Table I. Bonding energies for PTCDA-PTCDA, NTCDA-NTCDA, and PTCDA-NTCDA dimers are all plotted in the figure. It is apparent that the equilibrium distance in the stacking direction (assuming that the molecular planes of adjacent molecules are parallel, which is not the case for the NTCDA-NTCDA bulk crystal) are nearly always

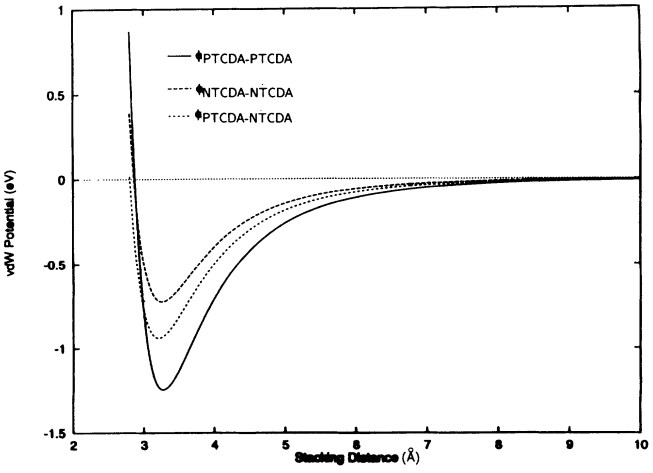

FIG. 2. The van der Waals potential as a function of interplanar stacking distance of a PTCDA dimer, a NTCDA dimer, and a PTCDA/NTCDA stack. For each curve, the two molecules are centered with respect to each other, with their molecular planes parallel.

TABLE I. vdW coefficients used in calculations.

Molecular bond	α (eV Å^6)	β (eV)	γ (Å)
H—H	1.96	432	4.52
C—H	5.51	3735	4.57
C—C	15.7	39 400	4.59
O—O	9.41	5860	4.59
C=O—O=C	16.1	9110	4.59
H—O	3.92	1160	4.57
H—O=C	5.29	1500	4.57
C—O	12.1	15 200	4.59
C—O=C	15.9	19 000	4.59

3.20–3.26 Å. Hence, to simplify the calculations made in the rest of this study, we fix the intermolecular stacking distance at 3.26 Å, which corresponds to the equilibrium PTCDA-PTCDA configuration. Note that this corresponds well with the experimentally determined value of 3.21 Å. We also find that the binding energy of the PTCDA dimer is approximately −1.3 eV, corresponding to 24 kcal/mol. This value is consistent with the sublimation energies of many aromatic molecules similar to PTCDA (e.g., anthracene[33]).

Once the stacking distance along the c unit-cell axis is fixed, the two molecules are translated in the x,y (base) plane with respect to each other to generate the energy surfaces for PTCDA and NTCDA dimers shown in Figs. 3(a) and 3(b), respectively. It is observed that the energy surfaces in both cases have two minima spaced at ±1.1 Å for the center of the PTCDA molecules, and ±1.0 Å for the NTCDA molecules. Note, however, that the minima in this latter case are very small compared with the energy when the two molecules are positioned directly over each other. The energy minima are displaced from the molecular center of mass, and are located along the long molecular axis. Hence the minimum energy is achieved when the molecules are offset by this distance, rather than when they lie directly above each other. This feature is experimentally observed in the PTCDA bulk structure, where the offset is at 0.9 Å as a result of the tilt of the molecular plane within the unit cell. Since the bulk molecular stacking habit of NTCDA is a herringbone configuration, we only include the planar stacking configuration here for reference. Thus, as the molecules become more circularly symmetric (as in the case of NTCDA), the lowest-energy close-packing arrangement results in herringbone, 3D stacking, whereas elongated molecules (e.g., PTCDA) prefer a planar-stacking configuration.

In further tests of this calculational method, we have also determined the energy of a 2D surface cell consisting of five PTCDA molecules placed in their characteristic base-centered rectangular configuration as observed by scanning tunneling microscopy (STM),[34] and shown in Fig. 4. For this calculation, all angles and dimensions are

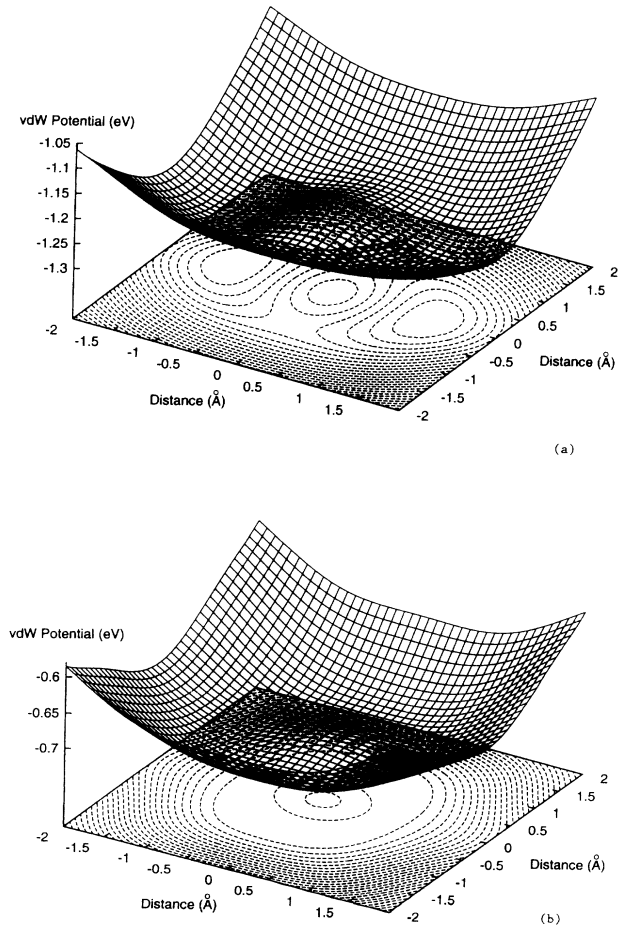

FIG. 3. The two dimensional dimer energy surface for (a) PTCDA and (b) NTCDA for the molecules oriented with their planes parallel.

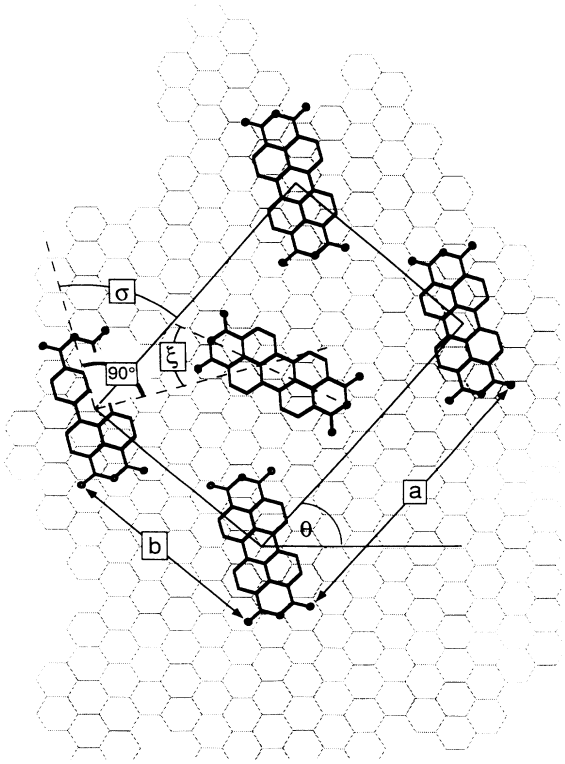

FIG. 4. Surface unit cell of PTCDA on a graphite substrate.

varied (including the relative angle of the central molecule with respect to the plane defined by the four corner molecules) to achieve the minimum-energy configuration, with the result shown in the figure. The angles and dimensions of the calculated surface unit cell agree to within 5% of the actual surface unit as determined from RHEED and STM including the following: (i) The surface unit cell is enlarged by 25% over that obtained for a bulk cell. This is clearly indicated in Fig. 5, where we plot energy vs distance of the corner molecules in both the x and y directions (given by ϕ_x and ϕ_y). The minimum energy corresponds to $x_{\min}=19.8\pm0.5$ Å and $y_{\min}=15.6\pm0.5$ Å, which accounts for the reconstructed surface dimensions of PTCDA observed by both STM and RHEED. The surface-cell minimum energy is obtained for all molecules in a coplanar configuration. By placing a second layer at 3.21 Å above the surface, the cell minimum energy is achieved only when $x_{\min}$ and $y_{\min}$ are decreased to values approaching their experimentally obtained bulk distances of $x_{\min}=17.34$ Å and $y_{\min}=11.96$ Å. (ii) When additional, out-of-plane molecules are added, the structure becomes slightly tilted as observed in the bulk. That is, as the surface molecules are pulled into close proximity by the out-of-plane molecules, the carboxyl groups approach to within the distance at which their repulsive cores force the molecules to tilt to allow for further cell shrinkage. Minimum energy is obtained when this tilt is 11°, according to observation. (iii) The central molecule of the surface cell is rotated to an angle of $\xi=0.48\pm0.02$ rad, also consistent with observation.

Both the theoretical and experimental[5,34,35] results for the bulk and surface unit cells are summarized in Table II, with the crystalline dimensional parameters defined in Figs. 1 and 4. In most cases, calculation and observation agree to $\leq 5\%$.

Having tested the accuracy of the model on known, bulk vdW molecular structures, we next considered the case of a monolayer grown on an incommensurate substrate. The first step in this procedure is to test the validity of the QE condition, i.e., that $\phi_{\text{intra}}'' \gg \phi_{\text{inter}}''$. Thus, in Fig. 6, we calculate the intermolecular potential, the force, and the elasticity of the NTCDA-NTCDA bond along two orthogonal axes which lie in the interface plane (corresponding to ϕ_{intra}, ϕ_{intra}', and ϕ_{intra}'', respectively). Due to the repulsive core energies, the lattices are rigid (i.e., ϕ_{intra}'' large) at the equilibrium separation of $x=8.7$ Å and $y=9.8$ Å. In contrast, in Fig. 7 we show results obtained for the NTCDA-PTCDA interface (i.e., ϕ_{inter}, ϕ_{inter}', and ϕ_{inter}'') with a calculated equilibrium intermolecular stacking separation of $d=3.2$ Å. The inset is a 2D plot of the energy surface obtained by translating a single NTCDA molecule across a PTCDA surface unit cell. The energy extrema are broad, implying that the NTCDA molecule can be displaced relative to the PTCDA substrate over more than 1 Å without significantly changing the total molecular energy. This is shown in more detail in Fig. 7, where we plot a cross section of the inset potential surface along one crystalline axis. Here, the broad minimum in the energy between NTCDA and PTCDA is apparent, with a very small shear stress (ϕ_{inter}'') near the minimum-energy position. Furthermore, the potential repeats with a period equal to the separation of the substrate molecules. However, this periodicity in the potential tends to vanish as the overlayer is extended over several unit cells due to their incommensurability with the substrate. Nevertheless, in comparing Figs. 6 and 7, it is apparent that the condition for QE ($\phi_{\text{intra}}'' \gg \phi_{\text{inter}}''$) is met by these molecules.

For comparison, in Fig. 8 we show the potential for a PTCDA molecule on a PTCDA surface. Once again, a broad minimum extending over more than 1 Å is observed. This broad minimum, which results in low shear stress at the interface (due to the small ϕ'') is a general feature of spatially extended planar molecules. It is this feature which we conclude is a key to QE growth, and hence should guide the choice of molecular structures used in achieving crystalline order. That is, the more ex-

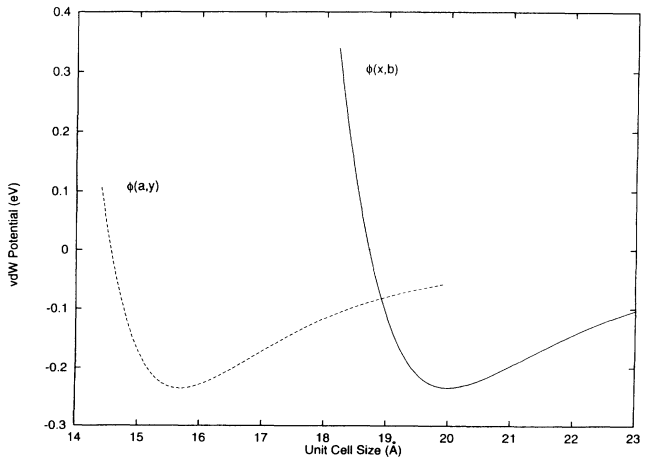

FIG. 5. Van der Waals potential ($\phi(x,y)$) for a PTCDA surface unit cell as a function cell dimension along the a and b directions (see Fig. 4). Minima at $a=15.6$ Å and $b=19.8$ Å correspond to the equilibrium cell dimensions.

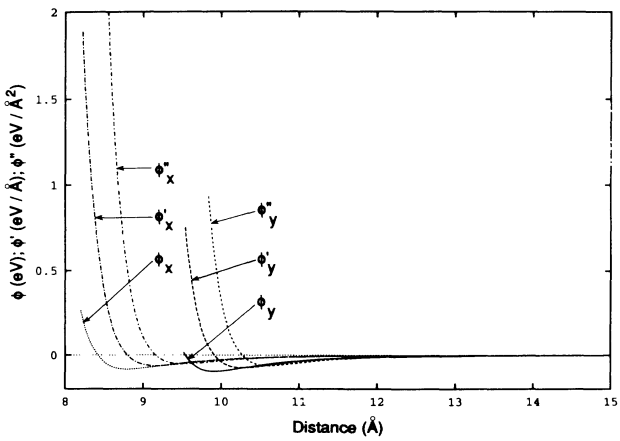

FIG. 6. The potential (ϕ), force (ϕ'), and elastic constant (ϕ'') of a NTCDA unit cell calculated along two cell directions (x,y).

TABLE II. PTCDA surface unit-cell parameters.

	a (Å)	b (Å)	σ (rad)	ξ (rad)	θ (rad)	Ref.
Theory	20.0±0.5	15.7±0.5	0.86±0.02	0.48±0.02	0.86±0.02	This work
STM	21.6±2.2	15.2±1.6	0.96±0.03	0.61±0.17	0.82±0.07	4
RHEED	22.4±1.0	16.0±1.0				3

PTCDA bulk unit-cell parameters

	Interplanar spacing (d) (Å)	Perp. molec. spacing (Å)	Molecular offset (Å)	Energy minimum (kcal/mol)
Theory	3.26	11.2	1.1	29
X ray	3.21	10.9	0.9	

tended molecules result in a broader energy minimum, and thus have a higher interfacial compressibility (i.e., lower elasticity, ϕ_{inter}''). Such molecules then can have a broader range of energy-equivalent positions, and therefore can result in the growth (under appropriate conditions) of an incommensurate overlayer with only a small interfacial energy, as required for order QE growth. Furthermore, this condition leads to the assumption of a rigid overlayer, relatively undistorted when placed in contact with the incommensurate substrate. This rigid overlayer approximation greatly simplifies calculations of the full QE structure, as will be shown below.

IV. ORIENTATION WITH RESPECT TO SUBSTRATE

The orientation of the adsorbed layer with respect to the substrate lattice can be defined in terms of an angle θ between primitive vectors in the two lattices. The value of θ leading to $\Phi'(\theta)=0$ and $\Phi''(\theta)>0$ corresponds to the equilibrium lattice configuration. Using the rigid-lattice approximation where the layers are translated with respect to each other without distortion, we have calculated θ, defined in Fig. 4, for a monolayer of PTCDA deposited on graphite. The results of this calculation are shown in Fig. 9. Here, a sufficiently large lattice (10×10 PTCDA unit cells) was considered in this calculation to ensure insensitivity of the result to layer boundaries and variations due to center-of-mass translation of the overlayer. We observe an energy minimum of -4 meV at $\theta_{\min}=0.85$ rad, where the energy axis in Fig. 9 is normalized to a single molecule of PTCDA adsorbed on graphite (-2.0 eV). This relatively small energy perturbation/molecule ($<0.3\%$) justifies the assumption that the overlayer is not influenced by the substrate, in contrast to atomic vdW systems (e.g., Ar on graphite) where the rotational energy is $\sim 5\%$ of the bond energy.[19] When summed over a large number of unit cells, however, the total rotational energy is substantial. Note that $\theta_{\min}$ is in good agreement with the experimental value[5,35] of $\theta=0.84\pm0.07$ rad (see Table II).

This calculation has been extended to study molecular interfaces consisting of NTCDA on a crystalline PTCDA substrate. Experimental evidence obtained for alternating multilayer stacks of these materials discussed in paper II and in previous work[2,5] imply that the layers form ordered crystalline organic multiple-quantum-well struc-

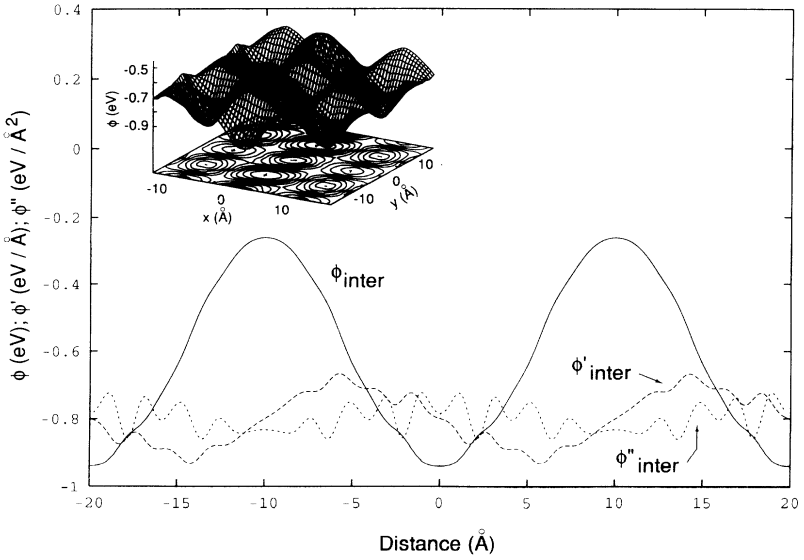

FIG. 7. The potential (ϕ), force (ϕ'), and elastic constant (ϕ'') of a molecule of NTCDA deposited on a PTCDA substrate lattice calculated along the PTCDA b direction. Here, ϕ' and ϕ'' are offset by -0.8 eV/Å and -0.8 eV/Å^2, respectively. Inset: Two-dimensional potential-energy surface of a molecule of NTCDA on a PTCDA substrate lattice. Note the broad potential minimum leading to a small shear stress, ϕ''.

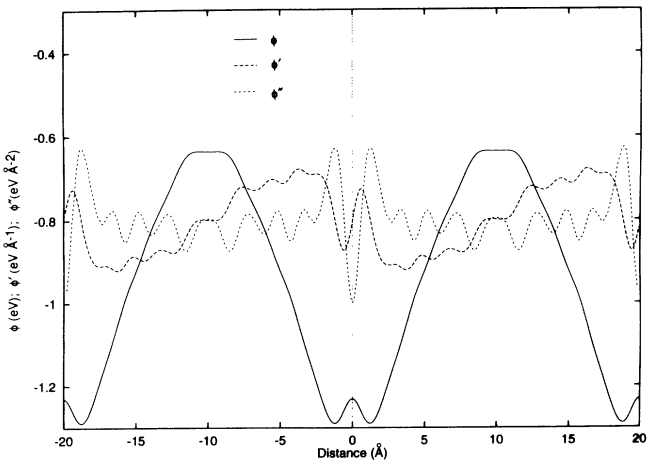

FIG. 8. The potential (ϕ), force (ϕ'), and elastic constant (ϕ'') of a molecule of PTCDA deposited on a PTCDA substrate lattice calculated along the PTCDA b direction.

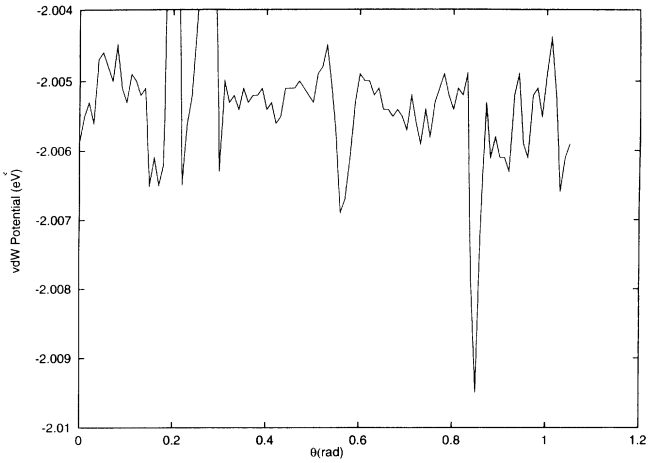

FIG. 9. Binding energy of a monolayer of PTCDA on a graphite substrate as a function of relative lattice angle, θ, as defined in Fig. 4. The vertical axis is the energy normalized to the binding energy per PTCDA admolecule.

tures. Due to the extended size of the molecules in both layers, and to the large number of pairwise atomic interactions between each molecule, the method outlined in Eq. (1) is calculationally impractical. We have, therefore, substantially simplified the procedure by replacing the $\sim 10^3$ atomic interactions between each NTCDA and PTCDA molecule with a *single*, elliptically symmetric potential assuming a fixed stacking distance. One such potential which fits well to molecules within a given layer is

$$\phi_{ij}(\theta)_{\mathrm{EP}} = -\alpha(\theta)/[r_{ij}-\delta(\theta)]^6 + \beta(\theta)\exp\{-\gamma(\theta)[r_{ij}-\delta(\theta)]\}, \quad r_{ij}-\delta(\theta)\geq 0\ , \tag{2}$$

where r_{ij} is now the center-center distance between *molecules*, $\delta(\theta)$ is the distance of closest approach of two adjacent molecules as calculated from their core repulsion, and the vdW constants are functions of the angle (θ) between unit cells in the overlayer and substrate. An alternative potential form which also provides a good fit to the atom-atom calculation, especially for molecules between planes, can be approximated by

$$\phi_{ij}(\theta)_{\mathrm{EP}} = -\phi_0\exp[-|x/\eta(\theta)|^{\varphi(\theta)} - |y/\kappa(\theta)|^{\lambda(\theta)}], \quad z=d\ , \tag{3}$$

where the distance in the z direction is held fixed at the interplanar spacing of d. The angular dependences of the parameters such as α, β, δ, etc. are simply and accurately (again to $\pm 5\%$) determined by translating one molecule over the substrate at a fixed vertical (equilibrium) distance in both the a and b crystalline directions while calculating the full atom-atom potential using Eq. (1). This provides values for α_a, α_b, β_a, β_b, γ_a, γ_b, δ_a, and δ_b, or similarly for the parameters in Eq. (3). To determine these parameters at other off-axis angles, we assume an ellipsoidal dependence, e.g.,

$$(\alpha(\theta)\cos\theta)^2/\alpha_a^2 + (\alpha(\theta)\sin\theta)^2/\alpha_b^2 = 1\ . \tag{4}$$

To illustrate the accuracy of this approximation, in Fig. 10(a) we plot the potentials calculated according to Eq. (3) along the x and y directions for the long axis of PTCDA perpendicular to that of NTCDA. Similarly, Fig. 10(b) shows the calculation for the long axes of the molecules oriented parallel to each other. As can be seen from the figure, the approximation is reasonably accurate, leading to only a 5% error in to the total binding energy of the PTCDA to NTCDA molecules along any particular crystalline axis, and for any relative orientation of the two molecules. Also, for NTCDA on PTCDA, we assume that the two basis molecules in the surface unit cells of both molecules are coplanar. This particular assumption has also been tested by allowing the NTCDA center-cell molecule to rotate about an axis in the plane of the surface cell. Rotation of the central molecule from the planar to the perpendicular configuration results in a $<5\%$ variation in cell energy, with the lowest energy achieved with all molecules in the cell lying in a coplanar manner. Hence we regard this approximation as adequate for the purposes of understanding the structure resulting from the layering of NTCDA on PTCDA.

Note that the ellipsoidal potential significantly simplifies numerical calculations while at the same time it is useful in treating the film structure from an analytical standpoint. While its use cannot lead to a precise

structural determination, it nevertheless yields a reasonably accurate quantitative description of the thin-film structure.

The curve line in Fig. 11 is obtained for a 1000-Å radius, rigid lattice of NTCDA (assuming circular boundary conditions) on a PTCDA substrate of similar size. The preferred orientation of the NTCDA lattice on PTCDA is $\theta_{min}=0.75\pm0.05$ rad, defined as the angle between the a axes of the two unit cells. The noise in the plot results from rounding errors and the limited size of the lattices considered. The minimum energy for PTCDA/NTCDA structures is broad (as compared to PTCDA on graphite) due to the large spatial extent of the molecules in the two layers. Nevertheless, the existence of such an energetically favored configuration (with -3.5 meV/molecule normalized to the PTCDA/NTCDA dimer binding energy of -0.90 eV) suggests that this materials combination will grow as an orientationally ordered, crystalline multilayer stack under the appropriate thermodynamic conditions, as has already been experimentally observed.[2,5,34]

From the foregoing results, we infer that the dependence of the orientation on molecular structure is implicit in the requirement that $\phi_{inter}'' \ll \phi_{intra}''$. Thus we have explored the generality of this growth configuration by examining the dependence of ϕ_{inter}'' on molecular shape for several common, vdW-bonded planar molecules. For this purpose, the energy of molecules in the polyacene series of benzene, naphthalene, pyrene, perylene, and coronene (with one, two, four, five, and seven carbon rings, respectively) "deposited" on a PTCDA substrate was studied. In Fig. 12, we show the calculated energy surfaces for single benzene and coronene molecules on a PTCDA substrate lattice. In these plots the energy (ϕ) is normalized to its minimum value ϕ_0. It is readily apparent that the energy minimum of the larger molecule is extremely broad and flat as compared to that of benzene. Hence, the shear stress (ϕ_{inter}'') for the coronene/PTCDA interface is much smaller than that of benzene, which should enhance the probability for successful QE growth of overlayers of the larger molecule.

In Fig. 13(a) we plot the normalized shear stress

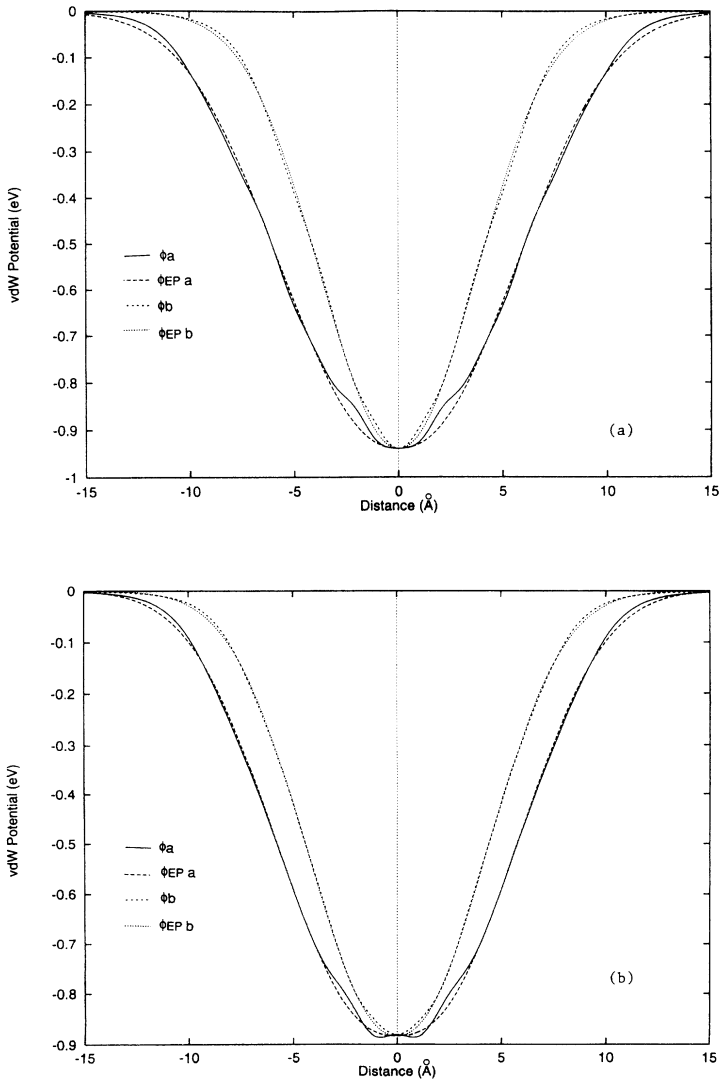

FIG. 10. The potential of a NTCDA molecule on a PTCDA substrate calculated for (a) the long axes of PTCDA and NTCDA oriented perpendicular to each other, and (b) parallel to each other. In both cases, the two molecular planes are parallel. Also shown is the potential calculated using the ellipsoidal molecule approximation and Eq. (3).

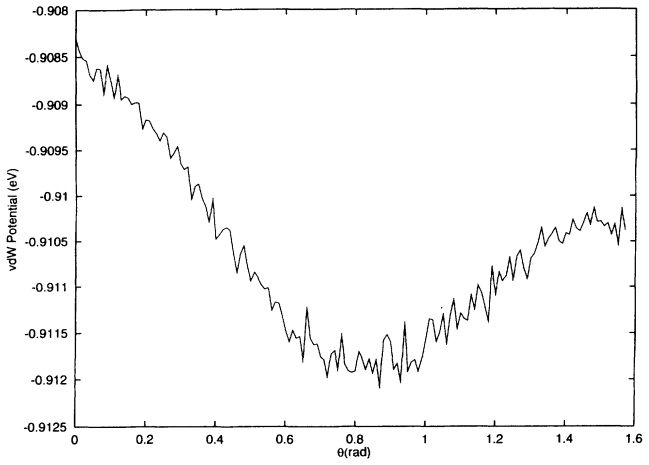

FIG. 11. Binding energy of a monolayer of NTCDA on a PTCDA substrate as a function of relative lattice angle, θ, as defined in Fig. 4 between the a axes of the two surface unit cells. The vertical axis is the energy normalized to the binding energy per NTCDA admolecule.

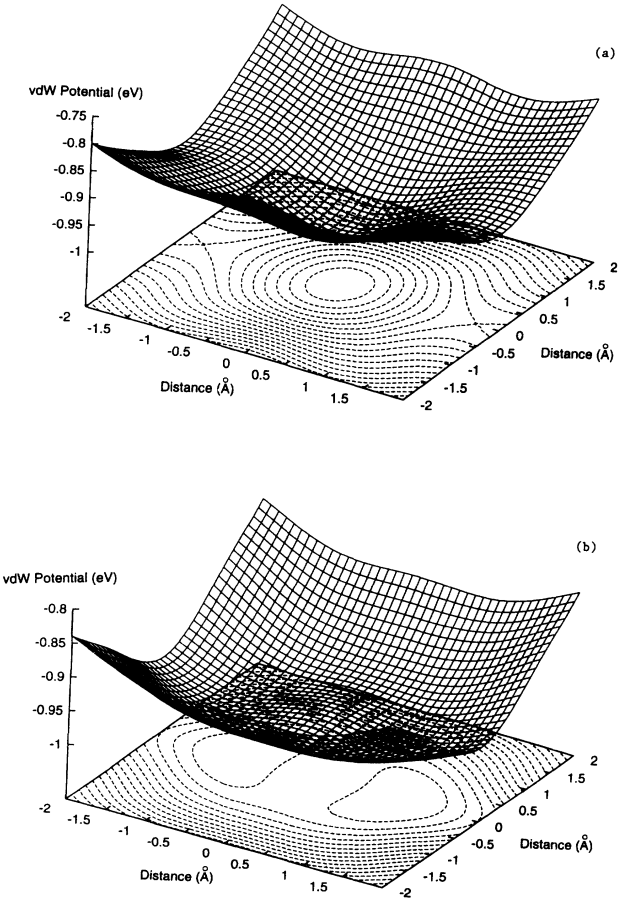

FIG. 12. Two-dimensional potential surface of (a) benzene and (b) coronene on a PTCDA substrate. Here the molecular planes of the substrate and admolecules are parallel.

$(\Delta^2\phi_{\text{inter}}/\Delta a^2)/\phi_0$ as a function of molecular moment of inertia, I_{mol} (normalized to benzene, I_{benz}). Here, $\Delta^2\phi/\Delta a^2$ is the energy difference divided by the surface area enclosing the energy 15% larger than its value at ϕ_0. Hence, $\Delta^2\phi_{\text{inter}}/\Delta a^2$ is the *incremental* shear stress which is numerically evaluated from the calculated values of $\phi(x,y)$. Dividing this value by ϕ_0 serves to normalize all of the data for comparison. Furthermore, the normalized moment of inertia of a particular molecule, $I_{\text{mol}}/I_{\text{benz}}$, is calculated about an axis perpendicular to, and centered in, the molecular plane of the admolecule. Hence, I provides a measure of the distribution of mass in the plane around the molecular center.

From Fig. 13(a), it is readily apparent that the normalized shear stress decreases monotonically with increasing molecular size, or number of carbon rings. Hence we expect that the ability to grow ordered, QE layers on PTCDA (or similar planar molecule) substrates increases as we progress from smaller (benzene) to larger, rounder molecules (coronene).

We note, however, that molecular shape (in comparison to the substrate molecule) also plays a significant role in the magnitude of the interlayer shear stress. This is shown in Fig. 13(b), where we repeat the calculation in Fig. 13(a) for a series of *linear* polyacenes deposited on graphite. Here the calculation is made for benzene, naphthalene, anthracene, tetracene, and pentacene (with one, two, three, four, and five rings, respectively). From this plot, we see that the shear stress decreases monotonically for the three smallest molecules, at which point it begins to increase for the larger molecules. The reason for this increase is that PTCDA has a perylene "core" which extends to only three rings. Hence, longer molecules (e.g., tetracene and pentacene) extend beyond the central molecule in the PTCDA surface cell, and overlap the spaces between adjacent substrate molecules. For the longest molecules, the rings can extend to the carboxyl end groups of adjacent substrate molecules. All of these effects will tend either to leave the shear stress unchanged (as in the case of tetracene-PTCDA), or even result in a small increase due to core repulsion from adjacent molecules (pentacene-PTCDA). While this plot does not indicate whether QE growth can be obtained for a given molecular combination, it does address the central condition under which QE is favored.

From the results discussed above, therefore, we conclude that QE is favored in systems where both the molecular shape and size of the substrate and overlayer molecules are approximately matched. While these conclusions only hold for planar molecules similar to the polyacenes studied, we nevertheless see that QE growth of ordered overlayers is a general property of a large range of planar molecules which are bonded primarily by vdW forces to the substrate.

The molecular film alignment to the substrate also must depend on the degree of symmetry of the substrate. For example, PTCDA, NTCDA, and CuPc lattices are monoclinic, and hence they have twofold symmetry. Hence, to ensure alignment of neighboring islands nucleated separately during the onset of growth, the substrate must also have a similar degree of symmetry. As

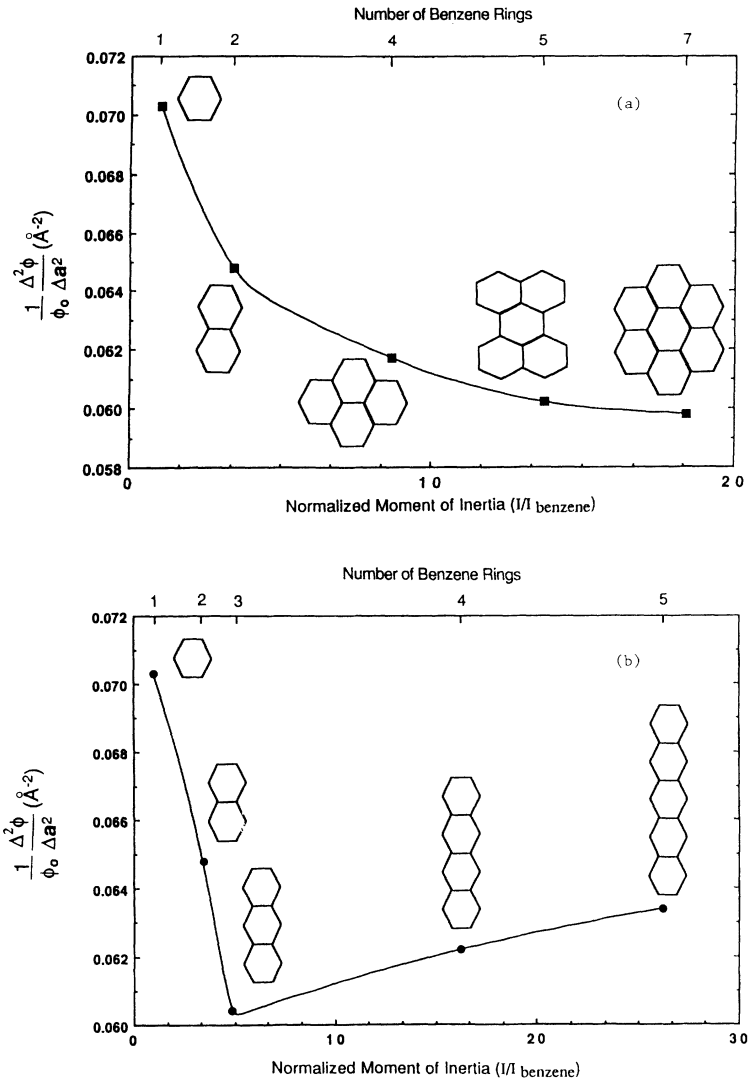

FIG. 13. Incremental shear stress for several molecules deposited on a PTCDA substrate lattice calculated as a function of molecular moment of inertia relative to benzene. The shear stress is normalized in each case to the minimum dimer potential energy ϕ_0. The moment of inertia is calculated about the axis perpendicular to, and centered in the molecular plane. (a) is for the molecules: benzene, naphthalene, pyrene, perylene, and coronene (with one, two, four, five, and seven carbon rings, respectively), and (b) is for the molecules: benzene, naphthalene, anthracene, tetracene, and pentacene (with one, two, three, four, and five carbon rings, respectively).

shown in the case of graphite[34] (which has sixfold symmetry), adjacent molecular islands nucleate with their principle axes rotated at angles of $m(\pi/3)$, where $m=0, \pm1, \pm2$, and ±3. This higher-order substrate symmetry therefore results in the formation of high-angle grain boundaries between islands. Other substrates with natural twofold symmetry (such as an organic thin film or other monoclinic lattice), or with a preferred twofold directionality (e.g., glass with a strain axis parallel to the surface,[2] semiconductor substrates oriented 1°–2° from the (100), narrow polymer stripes as used as waveguide buffer layers,[25] etc.) therefore can serve to avoid the occurrence of such grain boundaries.

V. DISCUSSION

It is useful to compare these results with those obtained using a model describing the "orientational epitaxy" of physisorbed inert gas atoms bonded by vdW forces onto lattice-mismatched graphite substrates. In that work,[19,20] it was proposed that mismatch between adsorbate and substrate results in small, periodic, static density variations (mass density waves, or MDW's) in the overlayer. Competition between longitudinal and transverse modes in these MDW's results in an energetically preferred angle ($\theta_{\min}$) between reciprocal-lattice vectors $\mathbf{G}$ and τ of the substrate and adsorbed layers, respectively. It can be shown that, for the special case of long MDW wavelength, $\theta_{\min}$ is determined by minimizing

$$\phi = -\sum_l \frac{\bar{u}_G^2[\mathbf{G}\cdot\varepsilon_l(\mathbf{G})]^2}{M\omega_l^2(\mathbf{G})}, \tag{5}$$

where $\bar{u}_G$ is the average displacement of a molecule in the overlayer, M is the molecular mass, and ε_l and ω_l are the eigenvectors and eigenvalues of the dynamical equation defined by $D(\omega_l)\lambda(\omega_l)=\omega_l\lambda(\omega_l)$. Here $D(\omega_l)$ is the dynamical matrix operator, and $\lambda(\omega_l)$ are the Bloch functions for the PTCDA surface lattice. This approach requires that the phonon-dispersion curves ($\omega_l(\mathbf{G})$) for the 2D lattices be calculated along the various crystal axes assuming vdW bonding described by Eq. (1). These calculations are difficult to check experimentally, and are

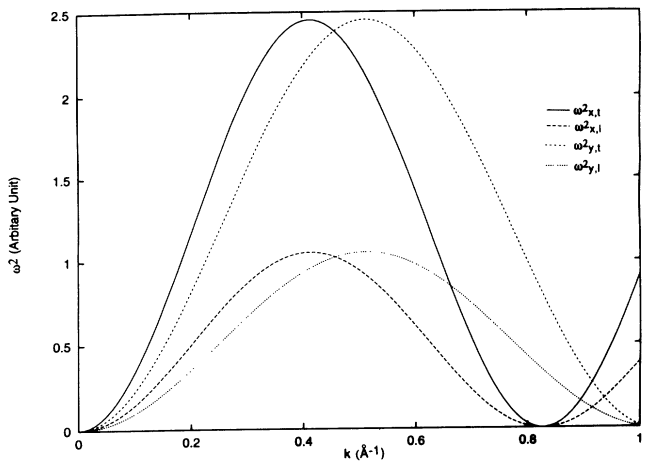

FIG. 14. Acoustical-phonon dispersion curves calculated for a PTCDA surface unit cell using the vdW potential.

particularly complex when applied to layers of low-order symmetry such as is typical of the monoclinic, base-centered lattices of NTCDA and PTCDA. Nevertheless, we have applied this technique to NTCDA/PTCDA assuming small equilibrium perturbations of the lattice molecules (i.e., the harmonic approximation). These calculations yield the two transverse and longitudinal acoustic modes shown in Fig. 14. Optical models are ignored in this calculation since ω for these terms is quite high, resulting in a small contribution to Eq. (5).

Summing the contributions from each mode gives the energy of the MDW shown in Fig. 15, where the energy axis is in arbitrary units. The several peaks correspond to the summation of phonon modes, ω_1, along the various crystal directions. These calculations indicate an energy minimum at $\theta_{\min}=0.65$ rad which is close to that obtained using Eq. (2). Note that we expect the contribution to the total layer energy due to this lattice distortion to be only a small effect in incompressible molecular lattices (where $M\omega_1^2$ is very large due to the large molecular mass and high vibrational energy), and thus should not alter the position of the NTCDA/PTCDA energy minimum from that shown in Fig. 11. We emphasize that the lattice distortion energy accounted for in Eq. (5) is a second-order effect in molecular systems, whereas in relatively compressible atomic vdW lattices (where M and ω_1 are small) this effect should dominate.

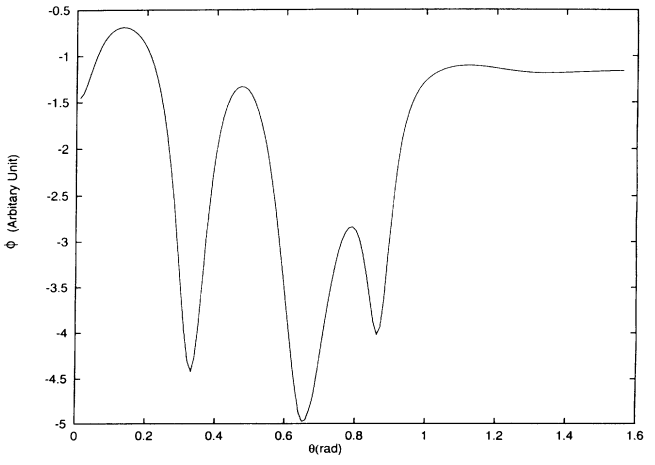

FIG. 15. Relative lattice energy for a NTCDA surface unit cell on NTCDA as a function of orientation, θ, as a result of strain induced in the adlayer. This energy is in addition to the rigid-lattice energy calculated in Fig. 11, and is expected to be small by comparison.

VI. CONCLUSIONS

In summary, we have introduced simple analytical techniques to understand the mechanisms underlying the formation of nearly defect-free layers of vacuum-deposited, organic molecular thin films on incommensurate substrate lattices. The study indicates that these quasiepitaxially ordered films are a general result of the flexibility of vdW bonds, along with the relatively large spatial extent of the planar-stacking molecules in the layers. This large spatial extent leads to an interface with a low shear stress, whereas as the layers themselves are relatively incompressible. We compared these results with experimental observation, as well as with previous models developed to understand the ordered arrangement of atoms physisorbed onto incommensurate substrate lattices. This comparison is studied further in paper II, where we present experimental data concerning the structure of monolayer and multilayer films of the compounds which are the focus of this work, i.e., PTCDA and NTCDA. It is found that the structures observed correspond well with theoretical predictions made here.

We note that while this theory predicts the favored, or minimum-energy, configuration of the grown layers, the degree and extent of layer ordering which is actually achieved depends critically on the thermodynamic conditions under which the growth occurs. These conditions are not predicted by this inherently static model, although we find that certain low-energy "thresholds" between structural isomorphs predicted in the theory suggest that growth at low temperatures is favorable for achieving uniform crystalline order, as has been experimentally observed in many cases. However, a nonstatic model is required for unambiguously determining the growth conditions which lead to maximum structural ordering. This model, which is beyond the scope of this work, is currently under investigation.

Finally, the results presented here suggest that large, vdW-bonded planar molecules lead themselves readily to ordered, QE growth on a variety of substrates without necessitating that the overlayer and substrate be lattice matched or commensurate. We note, however, that simply depositing large planar molecules on the substrates will not necessarily reduce the interfacial shear stress. An additional condition favoring QE growth is that the *shape* of the molecule (or the atomic mass distribution) be similar to the substrate molecular shape. That is, QE growth is favored for approximately round, planar mole-

cules deposited on similarly shaped molecules in the substrate. It is somewhat less favored (although not ruled out) in the case of long, linear molecules deposited on this same substrate structure. Low stress at the material interface, in all cases, should lead to structural ordering without sufficient strain to induce a high density of defects in the adlayers.

ACKNOWLEDGMENTS

The authors thank Dr. P. E. Burrows for many helpful discussions. We also gratefully acknowledge a grant from AFOSR (G. Pomrenke and C. Lee) and from the ARPA AMPP program, without whose support this work could not have been accomplished.

---

*On leave from the Department of Electrical Engineering, University of Southern California, Los Angeles, CA 90089.

[1]S. R. Forrest, M. L. Kaplan, and P. H. Schmidt, J. Appl. Phys. **56**, 543 (1984).

[2]F. F. So, S. R. Forrest, Y. Q. Shi, and W. H. Steier, Appl. Phys. Lett. **56**, 674 (1990).

[3]F. F. So and S. R. Forrest, Phys. Rev. Lett. **66**, 2649 (1991).

[4]S. Cincotti and J. B. Rabe, Appl. Phys. Lett. **62**, 3531 (1993).

[5]P. E. Burrows and S. R. Forrest, Appl. Phys. Lett. **62**, 3102 (1993).

[6]Y. Imanishi, S. Hattori, A. Kakuta, and S. Numata, Phys. Rev. Lett. **71**, 2098 (1993).

[7]U. Zimmermann, G. Schnitzler, N. Karl, and E. Umbach, Thin Solid Films **175**, 85 (1989).

[8]H. Hoshi, Y. Maruyama, H. Masuda, and T. Inabe, J. Appl. Phys. **68**, 1396 (1990).

[9]M. Mobus and N. Karl, Thin Solid Films **215**, 213 (1992).

[10]M. K. Debe, R. J. Poirier, and K. K. Kam, Thin Solid Films **197**, 335 (1991).

[11]K. Tanigaki, S. Kuroshima, T. W. Ebbesen, and T. Ichihashi, Mol. Cryst. Liq. Cryst. Sci. Technol. B: Nonlinear Opt. **2**, 179 (1992).

[12]T. Nonaka, Y. Mori, N. Nagai, T. Matsunobe, Y. Nakagawa, M. Saeda, T. Takahagi, and A. Ishitani, J. Appl. Phys. **73**, 2826 (1993).

[13]T. Minakata, H. Imai, M. Ozaki, and K. Saco, J. Appl. Phys. **72**, 5220 (1992).

[14]T. Kanetake, Y. Tomioka, S. Imazeki, and Y. Taniguchi, J. Appl. Phys. **72**, 938 (1992).

[15]C.-L. Cheng, S. R. Forrest, M. L. Kaplan, P. H. Schmidt, and B. Tell, Appl. Phys. Lett. **47**, 1217 (1985).

[16]D. Y. Zang, Y. Q. Shi, F. F. So, S. R. Forrest, and W. H. Steier, Appl. Phys. Lett. **58**, 562 (1990).

[17]F. F. So and S. R. Forrest, IEEE Trans. Electron. Dev. **36**, 66 (1988).

[18]C. W. Tang, Appl. Phys. Lett. **48**, 183 (1986).

[19]A. D. Novaco and J. P. McTague, Phys. Rev. Lett. **38**, 1286 (1977).

[20]J. P. McTague and A. D. Novaco, Phys. Rev. B **19**, 5299 (1979).

[21]C. Itoh, T. Miyazaki, K. Aizawa, H. Aoki, and M. Okazaki, J. Phys. C **21**, 4527 (1988).

[22]M. Hara, H. Sasabe, A. Yamada, and A. Garito, Jpn. J. Appl. Phys. **28**, L306 (1989).

[23]N. R. Armstrong, K. W. Nebesny, G. E. Collins, L.-K. Chau, P. A. Lee, C. England, D. Diehl, M. Douskey, and B. A. Parkinson, Thin Solid Films **216**, 90 (1992).

[24]G. E. Collins, V. S. Williams, L.-K. Chau, K. W. Nebesny, C. England, P. A. Lee, T. Lowe, Q. Fernandon, and N. R. Armstrong, Synth. Metals **54**, 351 (1993).

[25]Y. Zhang and S. R. Forrest, Phys. Rev. Lett. **71**, 2765 (1992).

[26]H. Reiss, J. Appl. Phys. **39**, 5045 (1968).

[27]J. H. van der Merwe, Philos. Mag. A **45**, 127 (1982).

[28]S. E. Harrison and J. M. Assour, J. Chem. Phys. **40**, 365 (1964).

[29]S. R. Forrest, M. L. Kaplan, P. H. Schmidt, T. Venkatesan, and A. J. Lovinger, Appl. Phys. Lett. **41**, 708 (1982).

[30]A. I. Kitaigorodsky, *Molecular Crystals and Molecules* (Academic, New York, 1973).

[31]A. Abe, R. L. Jernigan, and P. J. Flory, J. Am. Chem. Soc. **88**, 631 (1966).

[32]R. A. Scott and H. A. Scheraga, J. Chem. Phys. **42**, 2209 (1965).

[33]J. D. Cox and G. Pilcher, *Thermochemistry of Organic and Organometallic Compounds* (Academic, New York, 1970).

[34]S. R. Forrest, P. E. Burrows, E. I. Haskal, and F. F. So, following paper, Phys. Rev. B **49**, 11 297 (1994).